

# EXACT SOLUTION OF A LINEAR SPIN-ELECTRON CHAIN COMPOSED OF LOCALIZED ISING SPINS AND MOBILE ELECTRONS\*

J. ČISÁROVÁ<sup>†</sup>, J. STREČKA

Institute of Physics, Faculty of Science, P.J. Šafárik University  
Park Angelinum 9, 040 01 Košice, Slovakia

*(Received October 30, 2014; revised version received December 5, 2014)*

Exact solution of a coupled spin-electron linear chain composed of localized Ising spins and mobile electrons is found with the use of a transfer-matrix method. The ground-state phase diagram consists of three phases with different number of mobile electrons per unit cell, one of which is paramagnetic, one is ferromagnetic and one is antiferromagnetic. Thermal variations of specific heat with up to four distinct peaks are observed, while temperature dependences of isothermal electron compressibility reveal a round maximum at low temperatures when the investigated system is driven close to the ground-state boundary between the ferromagnetic and antiferromagnetic phase.

DOI:10.5506/APhysPolB.45.2093

PACS numbers: 75.10.Pq, 75.40.Cx, 05.50.+q, 64.70.qd

## 1. Introduction

Exactly soluble models have received a great amount of research interest since they can provide a deeper insight into many unusual cooperative phenomena [1–3]. Recently, a new class of exactly tractable models has been introduced by decorating the bonds of a simple lattice occupied by localized Ising spins with relatively small electron subsystems [4–8]. Theoretical study of this kind of spin-electron systems could provide an explanation of how the mobile electrons influence magnetic properties of various classes of materials with both localized and itinerant electrons [9–11].

---

\* Presented at the XXVII Marian Smoluchowski Symposium on Statistical Physics, “Fundamentals, Soft Matter and Biocomplexity”, Zakopane, Poland, September 22–26, 2014.

<sup>†</sup> Corresponding author: [jana.cisarova@upjs.sk](mailto:jana.cisarova@upjs.sk)

### 2. Model and method

In this paper, we will study a hybrid spin-electron model on a linear chain with localized Ising spins placed on its nodal sites and mobile electrons delocalized over the pairs of the decorating sites placed at each of its bonds (see Fig. 1 for schematic representation). The total Hamiltonian of the model can be defined as a sum over mutually commuting bond Hamiltonians  $\hat{\mathcal{H}} = \sum_{i=1}^N \hat{\mathcal{H}}_i$ , each containing all interaction terms involving the mobile electrons from  $i^{\text{th}}$  bond

$$\hat{\mathcal{H}}_i = -t \left( \hat{a}_{i,\uparrow}^\dagger \hat{b}_{i,\uparrow} + \hat{a}_{i,\downarrow}^\dagger \hat{b}_{i,\downarrow} + \hat{b}_{i,\uparrow}^\dagger \hat{a}_{i,\uparrow} + \hat{b}_{i,\downarrow}^\dagger \hat{a}_{i,\downarrow} \right) - \frac{J}{2} \left[ \sigma_i^z (\hat{n}_{ai,\uparrow} - \hat{n}_{ai,\downarrow}) + \sigma_{i+1}^z (\hat{n}_{bi,\uparrow} - \hat{n}_{bi,\downarrow}) \right]. \tag{1}$$

The symbols  $\hat{\alpha}_{i,\gamma}^\dagger$  and  $\hat{\alpha}_{i,\gamma}$  denote fermionic creation and annihilation operators for mobile electrons, which occupy decorating sites  $\alpha = \{a, b\}$  and have spin orientation  $\gamma = \{\uparrow, \downarrow\}$ . Moreover, the operator  $\hat{n}_{\alpha i, \gamma} = \hat{\alpha}_{i,\gamma}^\dagger \hat{\alpha}_{i,\gamma}$  with eigenvalues  $n_{\alpha i, \gamma} = \{0, 1\}$  represents the number operator for mobile electrons and the variable  $\sigma_i^z = \pm 1/2$  corresponds to the localized Ising spin placed on the  $i^{\text{th}}$  nodal lattice site. Finally, the parameter  $t$  represents the kinetic term for mobile electrons and the coupling constant  $J$  describes the Ising-type exchange interaction between the nearest-neighbour Ising spins and mobile electrons.

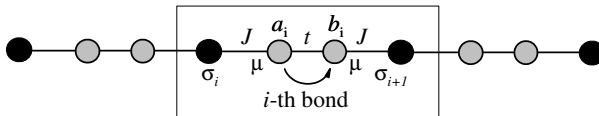


Fig. 1. A schematic representation of the investigated spin-electron system. Black circles denote nodal lattice sites occupied by the localized Ising spins, while grey circles denote decorating sites over which the mobile electrons are delocalized. A part of the system demarked by a rectangle is described by the bond Hamiltonian (1).

The grand-canonical partition function  $\Xi$  of the correlated spin-electron linear chain defined by the Hamiltonian (1) can be exactly calculated by following the procedure, which was elaborated in detail in our previous work [12]. For brevity, we will present in this paper just the crucial steps of the calculation procedure. Due to the commuting character of the bond Hamiltonians, the grand-canonical partition function can be partially factorized into the following product

$$\Xi = \sum_{\{\sigma_i\}} \prod_{i=1}^N \text{Tr}_i \exp \left( -\beta \hat{\mathcal{H}}_i \right) \exp \left( \beta \mu \hat{n}_i \right), \tag{2}$$

where the symbol  $\beta$  stands for the inverse temperature  $\beta = 1/T$  ( $k_B$  is set to unity). Symbol  $\sum_{\{\sigma_i\}}$  denotes summation over all possible configurations of nodal Ising spins,  $\text{Tr}_i$  stands for the trace over degrees of freedom of all mobile electrons delocalized over the  $i^{\text{th}}$  bond,  $\hat{n}_i = \sum_{\gamma=\{\uparrow,\downarrow\}}(\hat{n}_{ai,\gamma} + \hat{n}_{bi,\gamma})$  is the number operator corresponding to the total number of mobile electrons on  $i^{\text{th}}$  bond, and  $\mu$  stands for the chemical potential. After tracing out the degrees of freedom of the mobile electrons, the grand-canonical partition function  $\Xi$  depends solely on the localized Ising spins  $\{\sigma_i\}$  and this enables one to utilize the transfer-matrix method [1]. With the help of this method, the derivation of the exact solution for the grand-canonical partition function and the corresponding grand potential  $\Omega = -k_B T \lim_{N \rightarrow \infty} \ln \Xi / N$  is, in the thermodynamic limit, relatively straightforward (see Ref. [12] for more details). The grand potential  $\Omega$  can be subsequently used to calculate basic thermodynamic quantities such as the specific heat

$$C = -T(\partial^2 \Omega / \partial T^2)_z, \quad (3)$$

where  $z = e^{\beta\mu}$  is the fugacity, or the electron density

$$\rho = -(\partial \Omega / \partial \mu)_T \quad (4)$$

as well as the isothermal electron compressibility

$$\kappa_T = (\partial \rho / \partial \mu)_T / \rho^2. \quad (5)$$

### 3. Results and discussion

In this section, we will discuss in detail the most interesting results obtained for the investigated spin-electron linear chain. First, it should be mentioned that one can consider a ferromagnetic Ising interaction  $J > 0$  as well as non-positive values  $\mu \leq 0$  of the chemical potential throughout the rest of the paper without loss of generality, because the investigated model obeys in a zero field the time-reversal symmetry as well as the particle-hole symmetry. Moreover, the exchange coupling  $J > 0$  will be used for the definition of three dimensionless parameters: the dimensionless temperature  $T/J$ , the relative strength of the kinetic term  $t/J$ , and the reduced chemical potential  $\mu/J$ .

Let us explore in detail the ground-state phase diagram of the correlated spin-electron chain, which is depicted in the  $t/J - \mu/J$  plane in the upper panel of Fig. 2. It can be seen from this figure that the ground state of the studied spin-electron system consists of three different phases at which the total number of mobile electrons per couple of decorating sites is constant. Owing to the commutability of different bond Hamiltonians (1), the ground

state of the whole spin-electron chain can be written as tensor product over the lowest-energy eigenstates of the bond Hamiltonians (1). Spin arrangement in the respective ground states is schematically depicted in the lower panel of Fig. 2.

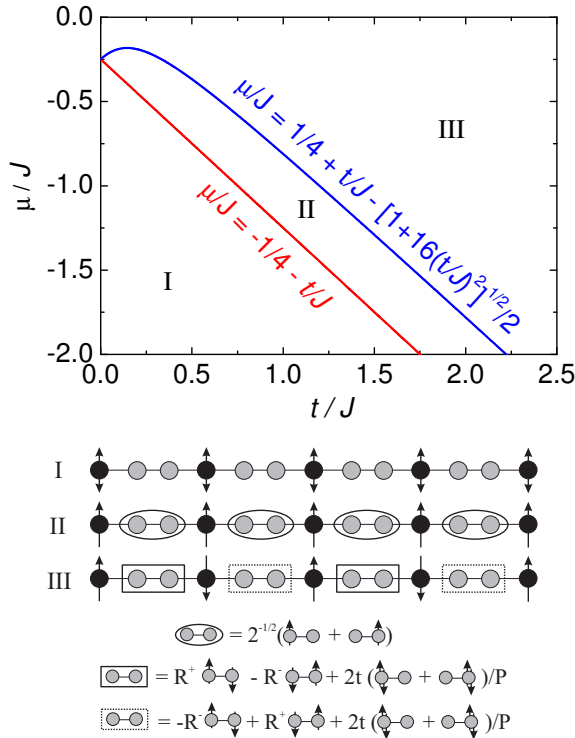


Fig. 2. Ground-state phase diagram and schematic representation of the ground-state phases of the studied spin-electron system. The lines correspond to the first-order phase transitions between the relevant ground states.

The ground state of the system for the lowest values of the chemical potential obeying the inequality  $\mu/J < -1/4 - t/J$  is the paramagnetic phase I

$$|I\rangle = \prod_{i=1}^N |\pm 1/2\rangle_{\sigma_i} |0, 0\rangle_i \tag{6}$$

with  $|0, 0\rangle_i$  denoting the vacuum state for mobile electrons from  $i^{\text{th}}$  bond and the energy  $E_I = 0$  per unit cell. This phase is disordered due to the absence of mobile electrons on the decorating sites, which consequently splits the investigated spin-electron chain into a set of non-interacting localized

Ising spins spatially separated by empty decorating sites. A more spectacular ground state can be detected for intermediate values of the chemical potential  $1/4 + t/J - \sqrt{1 + 16(t/J)^2}/2 > \mu/J > -1/4 - t/J$ , which stabilize the ferromagnetic phase II

$$|\text{II}\rangle = \prod_{i=1}^N |1/2\rangle_{\sigma_i} \frac{1}{\sqrt{2}} \left( \hat{a}_{i,\uparrow}^\dagger + \hat{b}_{i,\uparrow}^\dagger \right) |0, 0\rangle_i, \quad (7)$$

with energy  $E_{\text{II}} = -(J - 4t)/4$  per unit cell. Each pair of the decorating sites in the phase II is occupied by a single hopping electron, which is ferromagnetically coupled to its nearest-neighbour nodal Ising spins. The most remarkable ground state can be found for higher values of the chemical potential  $\mu/J > 1/4 + t/J - \sqrt{1 + 16(t/J)^2}/2$  in the antiferromagnetic phase III

$$\begin{aligned} |\text{III}\rangle = & \prod_{i=1}^{N/2} |1/2, -1/2\rangle_{\sigma_{2i-1}, \sigma_{2i}} \otimes \frac{1}{2} \left[ R_+ \hat{a}_{2i-1,\uparrow}^\dagger \hat{b}_{2i-1,\downarrow}^\dagger - R_- \hat{a}_{2i-1,\downarrow}^\dagger \hat{b}_{2i-1,\uparrow}^\dagger \right. \\ & \left. + \frac{2t}{P} \left( \hat{a}_{2i-1,\uparrow}^\dagger \hat{a}_{2i-1,\downarrow}^\dagger + \hat{b}_{2i-1,\uparrow}^\dagger \hat{b}_{2i-1,\downarrow}^\dagger \right) \right] |0, 0\rangle_{2i-1} \\ & \otimes \frac{1}{2} \left[ -R_- \hat{a}_{2i,\uparrow}^\dagger \hat{b}_{2i,\downarrow}^\dagger + R_+ \hat{a}_{2i,\downarrow}^\dagger \hat{b}_{2i,\uparrow}^\dagger + \frac{2t}{P} \left( \hat{a}_{2i,\uparrow}^\dagger \hat{a}_{2i,\downarrow}^\dagger + \hat{b}_{2i,\uparrow}^\dagger \hat{b}_{2i,\downarrow}^\dagger \right) \right] |0, 0\rangle_{2i} \end{aligned} \quad (8)$$

with new parameters  $P = \sqrt{J^2 + (4t)^2}$  and  $R_\pm = \frac{1}{2}(1 \pm J/P)$  and the energy  $E_{\text{III}} = -P/2$  per unit cell. Each pair of the decorating sites in the phase III is occupied by two mobile electrons, which rest in a quantum superposition of two antiferromagnetic states  $\hat{a}_{i,\uparrow}^\dagger \hat{b}_{i,\downarrow}^\dagger |0, 0\rangle_i$ ,  $\hat{a}_{i,\downarrow}^\dagger \hat{b}_{i,\uparrow}^\dagger |0, 0\rangle_i$  and two ionic states  $\hat{a}_{i,\uparrow}^\dagger \hat{a}_{i,\downarrow}^\dagger |0, 0\rangle_i$ ,  $\hat{b}_{i,\uparrow}^\dagger \hat{b}_{i,\downarrow}^\dagger |0, 0\rangle_i$ . It is quite evident that the hopping process of the mobile electrons gives rise to a Néel order of the localized Ising spins and consequently, the phase III has translationally broken symmetry. Let us point out here that the consideration of the antiferromagnetic coupling  $J < 0$  would not change the overall structure of the ground-state phase diagram. This change would just cause a trivial spin reversal of all nodal Ising spins in the respective ground-state phases (6)–(8), but all basic characteristics (thermodynamic quantities like electron density, entropy, specific heat, compressibility) will remain invariant under this transformation.

Thermodynamic properties of the hybrid spin-electron model will be illustrated by considering particular cases with fixed value of the reduced chemical potential  $\mu/J$  and the value of kinetic term  $t/J = 1.0$ . First, the

thermal variations of electron density are depicted in Fig. 3. It can be seen from this figure that the low-temperature limits of the electron density are in agreement with the number of electrons per unit cell, as discussed previously by the ground-state analysis in dependence on the selected value of the chemical potential. Obviously, the most remarkable thermal dependences with a sudden increase (decrease) can be observed near the critical values of the chemical potential, which determine the phase boundaries between the phases I–II and II–III, respectively.

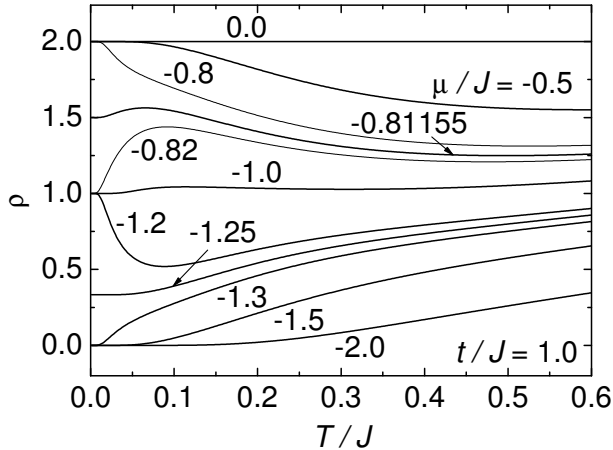


Fig. 3. Thermal dependences of the electron density for fixed value of the kinetic term  $t/J = 1.0$  and various values of the chemical potential  $\mu/J$ .

Next, thermal dependences of the isothermal compressibility  $\kappa_T$  are depicted in Fig. 4. Figure 4 (a) depicts thermal variations of isothermal compressibility for the values of the chemical potential  $\mu/J = -2.0, -1.0$  and  $-0.5$ , which display quite typical thermal dependences of the isothermal compressibility provided that the ground state is formed by the phases I, II and III, respectively. On the other hand, as one can see from Fig. 4 (b), the reduced isothermal compressibility  $\kappa_T$  starts from zero, then it shows a round maximum at relatively low temperatures before it repeatedly tends to zero at high enough temperatures whenever the chemical potential  $\mu/J$  is selected in a vicinity of the ground-state boundary between the ferromagnetic phase II and antiferromagnetic phase III.

Finally, the thermal dependences of the specific heat are displayed in Fig. 5. The double-peak structure of the specific-heat curves can be observed in Fig. 5 (a), which shows typical temperature dependences when the chemical potential  $\mu/J = -1.0$  and  $0.0$  drives the ground state either towards the ferromagnetic phase II or the antiferromagnetic phase III, respectively. The most interesting thermal dependences can be seen in Fig. 5 (b) for the values

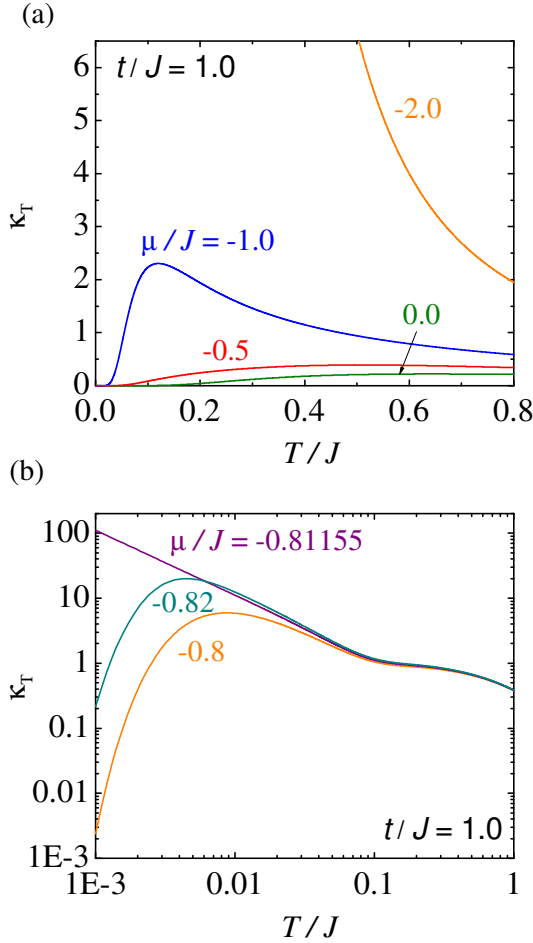


Fig. 4. Thermal dependences of the isothermal compressibility for the fixed value of the reduced kinetic term  $t/J = 1.0$  and several values of the chemical potential  $\mu/J$ . Figure 4 (b) shows dependences near the ground-state boundary between the phases II and III in a logarithmic scale.

of the chemical potential  $\mu/J$ , which are close enough to the ground-state phase boundary between the phases II and III. As one can see, temperature dependences with up to four distinct peaks can be observed.

In conclusion, the exact solution for the coupled spin-electron system on a linear chain with localized Ising spins and mobile electrons was found with the use of the transfer-matrix method. The ground state of this model comprises of one paramagnetic, one ferromagnetic and one antiferromagnetic phase, which differ in the number of mobile electrons per unit cell as

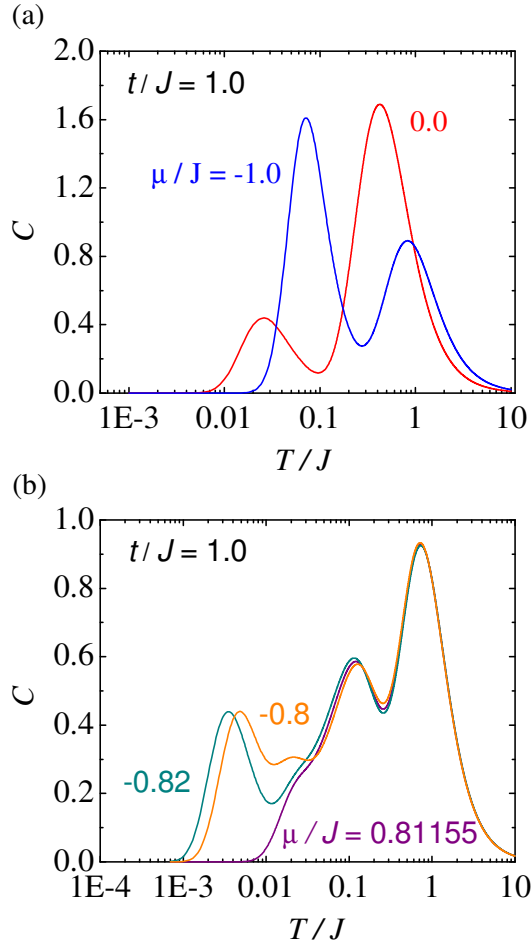


Fig. 5. Semilogarithmic thermal dependences of the specific heat for the fixed value of the kinetic term  $t/J = 1.0$  and various values of the chemical potential  $\mu/J$ .

well as respective spin arrangement of the localized Ising spins. Thermodynamic properties of the model were studied, whereas the most interesting thermal dependences of the isothermal compressibility and specific heat can be observed when the chemical potential drives the investigated correlated system close to the ground-state boundary between the ferromagnetic and antiferromagnetic phase.

This work was financially supported by the Slovak Research and Development Agency under the contract No. APVV-0097-12 and by the grant No. VVGS-PF-2014-434.

REFERENCES

- [1] R.J. Baxter, *Exactly Solved Models in Statistical Mechanics*, Academic Press, London 1982.
- [2] P. Fazekas, *Lecture Notes on Electron Correlation and Magnetism*, World Scientific, Singapore 1999.
- [3] F.H.L. Essler *et al.*, *The One Dimensional Hubbard Model*, Cambridge University Press, 2005.
- [4] M.S.S. Pereira, F.A.B.F. de Moura, M.L. Lyra, *Phys. Rev.* **B77**, 024402 (2008).
- [5] J. Strečka, A. Tanaka, L. Čanová, T. Verkholyak, *Phys. Rev.* **B80**, 174410 (2009).
- [6] L. Gálisová, J. Strečka, A. Tanaka, T. Verkholyak, *J. Phys.: Condens. Matter* **23**, 175602 (2011).
- [7] B.M. Lisnii, *Low Temp. Phys.* **37**, 296 (2011).
- [8] O. Rojas, S.M. de Souza, N.S. Ananikian, *Phys. Rev.* **E85**, 061123 (2012).
- [9] L.J. de Jongh, in: *Magnetic Properties of Layered Transition Metal Compounds*, edited by L.J. de Jongh, Kluwer Academic Publishers, Dordrecht 1990.
- [10] J. Jensen, A.R. Mackintosh, *Rare Earth Magnetism — Structures and Excitations*, Clarendon Press, Oxford 1991.
- [11] K.H.J. Buschow, *Handbook of Magnetic Materials*, Vol. 13, Elsevier, Amsterdam 2001.
- [12] J. Čisárová, J. Strečka, *Phys. Lett.* **A378**, 2801 (2014).